

A Methodology to Evaluate Wireless Technologies for the Smart Grid

Michael Souryal, Camillo Gentile, David Griffith, David Cypher, and Nada Golmie

National Institute of Standards and Technology
Emerging and Mobile Network Technologies Group
Gaithersburg, Maryland, USA

{michael.souryal,camillo.gentile,david.griffith,david.cypher,nada.golmie}@nist.gov

Abstract—This paper presents a methodology for assessing the suitability of various wireless technologies for meeting the communication requirements of Smart Grid applications. It describes an approach for translating application requirements to link traffic characteristics, determining the transmission range or coverage area of a wireless technology, and modeling the link layer to obtain performance measures such as message reliability, delay, and throughput. To illustrate the use of this approach, we analyze the performance of three representative application use cases over an IEEE 802.11 link.

I. INTRODUCTION

While there is general agreement on the need for communication networks to support a two-way flow of information between the various entities in the electric grid, there is still much debate on what networking technology should be used by each Smart Grid application domain and how it should be implemented. Using wireless communications has many benefits, including untethered access to information, support for mobility, reduced cost and complexity associated with wiring and maintenance, and support for interoperability. While many of these benefits apply to the grid, there are a number of challenges that remain. At the heart of the debate are questions regarding network performance, suitability, interoperability, and security. Can existing networking technologies and, more specifically, wireless communication systems support the communication requirements specific to the Smart Grid? How does one choose between different technologies with very different characteristics? Are there any implications for using a certain type of wireless technology in a certain environment? Are there any interference issues and what are their impact on the overall system performance? These questions are currently being addressed within the National Institute of Standards and Technology (NIST) Framework and Roadmap for Smart Grid Interoperability Standards, which identifies at least three priority action plans (PAPs) related to networking, and one specific to wireless communications, known as PAP#2 [1].

The full description of the procedures used in this guide requires the identification of certain commercial products and their suppliers. The inclusion of such information should in no way be construed as indicating that such products or suppliers are endorsed by NIST or are recommended by NIST or that they are necessarily the best materials, instruments, software or suppliers for the purposes described.

Given that a starting point for this effort was to consider what constitutes Smart Grid specific applications and their communication requirements, NIST created a template for cataloging applications' communication requirements. This template contains two main sections: one for characterizing the user applications, and the other for characterizing the physical devices (actors) that carry out application functions. In addition, NIST devised an evaluation framework to model wireless technology performance in various operational scenarios. This article is primarily concerned with this evaluation framework. Example Smart Grid applications and use cases are drawn from the UCAiug OpenSG (SG-Network) [2] application requirements.

A complete evaluation would also include an analysis of security issues, such as those identified in a recent U.S. Department of Energy study [3]. An approach to such an analysis, however, is outside the scope of this paper.

The remainder of this paper is organized as follows. Section II provides an overview of the evaluation framework proposed by NIST. Section III presents a procedure to convert the application requirements into useful data for telecommunications modeling and provides an example. Section IV describes an approach for analysis of the coverage limits of a wireless technology, the results of which can be used to guide network planning. Based on the input from the application requirements and the topology implications of the coverage analysis, Section V analyzes communications performance using a model of a specific wireless standard, IEEE 802.11, as an illustrative example.

II. EVALUATION METHODOLOGY

The methodology adopted in this paper to analyze the Smart Grid segments the network into a collection of telecommunication links. This enables studying the protocol layers of the wireless links individually. Here we concentrate only on the Physical (PHY) and Medium Access Control (MAC) layers; the other layers in the protocol stack are represented only in terms of the overhead they contribute to the message size. Fig. 1 illustrates the building blocks of our methodology. The PHY and MAC models process a set of input parameters capturing the environment, the Smart Grid application requirements, and the wireless technology used over the link; the

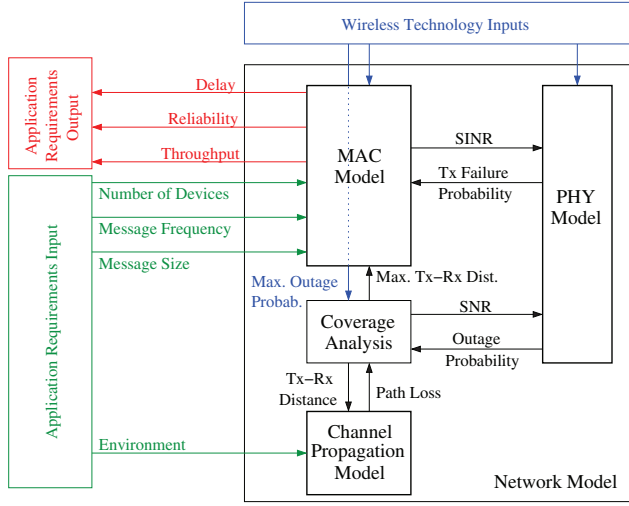


Fig. 1. Building blocks of modeling methodology

models return a set of metrics to gauge the performance of the technology in application to the Smart Grid.

At the most primitive level of the methodology, the environment (residential/industrial/indoor/outdoor/etc.) in which the link must operate is characterized by a path loss channel propagation model. Specifically, the path loss exponent quantifies the harshness of the environment in terms of the rate at which the signal loses strength as a function of transmitter-receiver (TX-RX) distance. The channel propagation model, together with the wireless technology parameters, feeds into the coverage analysis described in detail in Section IV. Using the PHY layer model, the coverage analysis determines the maximum TX-RX distance that satisfies a constraint on the outage probability, after accounting for shadowing and small-scale fading. In addition, the PHY model provides the MAC model with the probability that a transmission will fail when subject to interference from other devices within the same coverage area. A transmission fails when the received signal-to-interference-and-noise ratio (SINR) lies below a required level specific to the wireless technology under consideration.

The MAC model, summarized in Section V, is described in detail in [4]. The input parameters to the MAC model from the application requirements translate into the number of devices in a coverage area and the traffic flow on the links; the latter is defined by the message arrival rate and the message size. In addition, input parameters specific to the wireless technology define the message overhead. The MAC model outputs the reliability, delay, and throughput of the link. The reliability is defined as the probability that, once a message is generated by the transmitting device, it is successfully received by the intended device. The delay is the mean time required to complete the sequence of events, and the throughput is the bit transfer rate over the link.

III. LINK TRAFFIC ANALYSIS

Using the application requirements that cover the various Smart Grid domains, this section describes a procedure to

convert these requirements into link traffic data characteristics for telecommunications modeling and provides an example.

A. Link Traffic Characteristics

Given a Smart Grid network link topology, the application requirements can be converted to link requirements in order to analyze the traffic flow on each link. A link (j, k) is denoted by the downlink message flow from actor j to actor k ; in general, the links are asymmetric and so let link (k, j) denote the uplink flow from k to j . The traffic flow on each link is quantified by the *aggregate link message rate* λ_{jk}^{agg} and the *average link message size* L_{jk}^{avg} , after accounting for all the relevant applications specified in the requirements matrix. Assuming application traffic generated by different sources is modeled as independent Poisson processes with respective generation rates λ_{app}^i and message sizes L_{app}^i , the conversion can be performed as follows: for each of the applications indexed $i = 1, \dots, N_{app}$, where N_{app} is the total number of applications, set the boolean variable b_{jk}^i to 1 if the application traffic flows on link (j, k) and 0 otherwise. Then the probability p_{jk}^i that a message on link (j, k) originates from application i is [5]

$$p_{jk}^i = \frac{b_{jk}^i \lambda_{app}^i}{\lambda_{jk}^{agg}}, \quad (1)$$

where the aggregate message rate on link (j, k) can be expressed as

$$\lambda_{jk}^{agg} = \sum_{i=1}^{N_{app}} b_{jk}^i \lambda_{app}^i. \quad (2)$$

Then the average message size on link (j, k) follows as

$$L_{jk}^{avg} = \sum_{i=1}^{N_{app}} p_{jk}^i L_{app}^i. \quad (3)$$

B. Example

Out of the many high level application use cases identified to date, few have been quantified enough to be evaluated. We consider the three use cases defined in [2]: Service Switch (SS), Meter Reading (MR), and Plug in Hybrid Electric Vehicle (PHEV). Considering all the applications associated with these use cases in the requirements matrix, we examine the aggregate flow on a single link in the network between the Advanced Metering Infrastructure (AMI) Headend and the Data Aggregation Point (DAP), as an example. Nine applications send traffic across this link. The nine message generation rates λ_{app}^i and application message sizes L_{app}^i appear in Fig. 2. They are used to compute the aggregate link arrival rate λ_{jk}^{agg} and the average link message size L_{jk}^{avg} through (2) and (3) as 6.7×10^{-5} events per electric smart meter (emeter) per second and 197.1 bytes, respectively. We can repeat this process for all the links between the actors in the example link topology shown in Fig. 3, resulting in the link requirements matrix shown in Table I. Each link corresponds

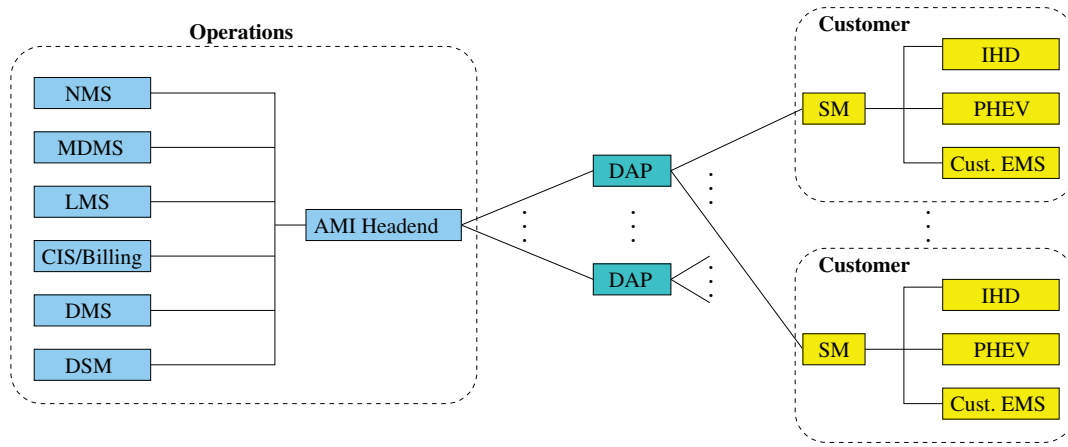


Fig. 3. Example link topology

TABLE I
RESULTING LINK REQUIREMENTS MATRIX

Uplink l_{kj}	λ_{kj}^{agg} (msg/s)	L_{kj}^{avg} (bytes)	Downlink l_{jk}	λ_{jk}^{agg} (msg/s)	L_{jk}^{avg} bytes
Cust. EMS \rightarrow SM	1.2×10^{-4}	25	SM \rightarrow Cust. EMS	$1.2 \times 10^{-7}/\text{emeter}$	50
PHEV \rightarrow ESI-SM	$2.4 \times 10^{-4}/\text{phev}$	97.6	ESI-SM \rightarrow PHEV	9.3×10^{-5}	177.5
IHD \rightarrow SM	1.2×10^{-4}	25	SM \rightarrow IHD	1.2×10^{-7}	50
SM \rightarrow DAP	$1.1 \times 10^{-4}/\text{emeter}$	2017.4	DAP \rightarrow SM	$1.8 \times 10^{-6}/\text{emeter}$	25
DAP \rightarrow AMI Headend	$1.3 \times 10^{-4}/\text{emeter}$	842.5	AMI Headend \rightarrow DAP	$6.7 \times 10^{-5}/\text{emeter}$	197.1
AMI Headend \rightarrow CIS/Billing	$6.3 \times 10^{-7}/\text{emeter}$	96.1	CIS/Billing \rightarrow AMI Headend	$1.5 \times 10^{-6}/\text{emeter}$	25
AMI Headend \rightarrow LMS	$1.4 \times 10^{-5}/\text{emeter}$	99.9	LMS \rightarrow AMI Headend	$6.9 \times 10^{-6}/\text{phev}$	255
AMI Headend \rightarrow MDMS	$1.3 \times 10^{-5}/\text{emeter}$	107.0	MDMS \rightarrow AMI Headend	$1.3 \times 10^{-5}/\text{emeter}$	25
AMI Headend \rightarrow NMS	$4.4 \times 10^{-7}/\text{emeter}$	50			
AMI Headend \rightarrow DMS	$4.6 \times 10^{-8}/\text{phev}$	50			
AMI Headend \rightarrow DSM	$6.3 \times 10^{-7}/\text{phev}$	96.3			

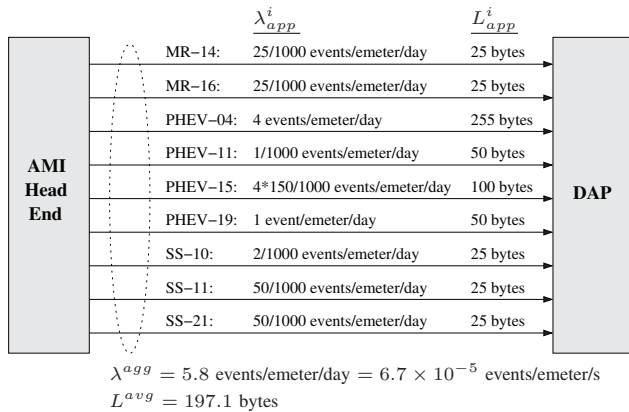


Fig. 2. AMI Headend to DAP link

to a row in the matrix. Note that the matrix distinguishes between downlink and uplink flows.

IV. COVERAGE ANALYSIS

The purpose of the coverage analysis is to predict the maximum range of a wireless technology for a given outage probability and a specified set of operating parameters. The range of a wireless technology can help to determine its suitability for linking a particular pair of actors, the number

of actors it can support in a point-to-multipoint arrangement, and the resulting network topology.

The outage criterion is the probability that the wireless transmitter-receiver link is not operational. It is expressed in terms of a probability because of the unpredictable behavior of RF propagation, which is often modeled as a stochastic process when accounting for the possible losses due to obstructions (shadowing) and reflections (multipath fading).

In the context of a point-to-multipoint wireless technology, coverage is often analyzed in terms of the maximum cell radius that a base station (BS) or access point (AP) can support. Within the cell, the outage probability varies, generally increasing as a terminal approaches the cell edge. In the analysis below, the outage criterion is expressed in terms of the *average outage probability*, averaged over all locations in the coverage area. Thus, a reported outage probability of 1%, for example, means that a terminal located at a random point in the cell has a 1% chance of being in outage.

We define the outage probability as the probability that the received signal-to-noise-ratio (SNR) is below the required SNR to operate the link. The required SNR depends on the wireless technology under consideration and serves as an input to the analysis. The *received SNR* is modeled as having a deterministic component, based on transmitter-receiver separa-

TABLE II
PATH LOSS PARAMETERS AT 2.4 GHz FOR SEVERAL ENVIRONMENTS

Environment	PL_0 (dB)	n_0	d_1 (m)	n_1	σ (dB)
Indoor residential LOS	16.3	4.2	N/A	N/A	2.4
Indoor residential NLOS	12.5	4.2	11	7.6	3.0
Indoor industrial NLOS	29.4	3.4	N/A	N/A	6.3
Outdoor urban-canyon NLOS	21.3	3.6	N/A	N/A	7.4
Indoor-outdoor convention center NLOS	4.2	2.6	100	5.7	4.6

tion distance, and random components due to shadowing and fading. For the distance-based deterministic component, we assume a dual-slope model of path loss versus distance. For the shadowing, we assume a lognormal distribution, and for the fading, we assume a Nakagami distribution of the fading envelope [6].

A. Nominal Received SNR

The deterministic component of the received SNR, or the nominal SNR at some transmitter-receiver distance d in the absence of fading and shadowing, can be evaluated using a link budget approach. In terms of the commonly used E_b/N_0 , the ratio of the received energy per bit to the power spectral density of the noise, it is modeled in decibels as

$$\overline{\left(\frac{E_b}{N_0}\right)}_{\text{rx,dB}}(d) = EIRP_{\text{dBm}} + G_{\text{r,dBi}} - PL_{\text{dB}}(d) - L_{\text{s,dB}} - N_{0,\text{dBm/Hz}} - R_{\text{b,dB-b/s}} \quad (4)$$

where $EIRP_{\text{dBm}}$ is the effective isotropic radiated power from the transmitter (dBm), $G_{\text{r,dBi}}$ is the receiver antenna gain (dBi), $PL_{\text{dB}}(d)$ is the path loss at distance d (dB), $L_{\text{s,dB}}$ is the cumulative system loss due to cabling or other implementation losses (dB), $N_{0,\text{dBm/Hz}}$ is the power spectral density of the noise (dBm/Hz)—computed as $30 + \log_{10}(kT_0F)$ where k is Boltzmann's constant (J/K), T_0 is the temperature (K), and F is the receiver's noise figure—and $R_{\text{b,dB-b/s}}$ is the physical layer information data rate (dB-b/s).

Using the dual-slope path loss model, the term for path loss with distance in (4) is calculated as

$$PL_{\text{dB}}(d) = PL_0 + \begin{cases} 10n_0 \log_{10} d & ; d \leq d_1 \\ 10n_0 \log_{10} d_1 + 10n_1 \log_{10} (d/d_1) & ; d > d_1 \end{cases}$$

where n_0 and n_1 are the path loss exponents of the dual-slope model, d_1 is the breakpoint distance (m) from path loss exponent n_0 to n_1 , and PL_0 is the reference path loss at 1 m. Table II lists values for these parameters that were extracted from measurements made at 2.4 GHz in various environments [7]–[10]. Environments in Table II for which there was no breakpoint (i.e., for which the path loss can be modeled with a single slope) have “N/A” listed for d_1 and n_1 .

B. Calculating Outage Probability

The outage probability at distance d is the probability that the received SNR, $(E_b/N_0)_{\text{rx}}(d)$, is less than the required SNR, $(E_b/N_0)_{\text{req}}$:

$$\begin{aligned} P_{\text{out}}(d) &= \Pr \left[\left(\frac{E_b}{N_0}\right)_{\text{rx,dB}}(d) < \left(\frac{E_b}{N_0}\right)_{\text{req,dB}} \right] \\ &= \Pr \left[\overline{\left(\frac{E_b}{N_0}\right)}_{\text{rx,dB}}(d) + X < \left(\frac{E_b}{N_0}\right)_{\text{req,dB}} \right] \\ &= F_X \left[\left(\frac{E_b}{N_0}\right)_{\text{req,dB}} - \overline{\left(\frac{E_b}{N_0}\right)}_{\text{rx,dB}}(d) \right] \quad (5) \end{aligned}$$

where $X = X_{\text{s,dB}} + X_{\text{f,dB}}$ is the combined random attenuation due to shadowing and fading, and $F_X(x)$ is the cumulative distribution function (cdf) of the random variable X .

Based on the assumption of lognormal shadowing, the shadowing attenuation $X_{\text{s,dB}}$ is modeled as a zero-mean Gaussian random variable with standard deviation σ . (Table II lists values of σ obtained by measurement in various environments.) In the presence of shadowing alone (i.e., $X = X_{\text{s,dB}}$), the cdf of X is

$$F_X(x) = 1 - \frac{1}{2} \operatorname{erfc} \left(\frac{x}{\sigma\sqrt{2}} \right)$$

where $\operatorname{erfc}(\cdot)$ is the complementary error function.

Based on the assumption of Nakagami- m fading, the fading attenuation X_f is modeled as a unit-mean Gamma-distributed random variable. In the presence of fading alone (i.e., $X = X_{\text{f,dB}} = 10 \log_{10} X_f$), the cdf of X is

$$F_X(x) = P(mx, m)$$

where $P(x, a) = \frac{1}{\Gamma(a)} \int_0^x e^{-t} t^{a-1} dt$ is the incomplete gamma function (lower regularized).

In the presence of combined lognormal shadowing and Nakagami fading ($X = X_{\text{s,dB}} + X_{\text{f,dB}}$), the cdf of X can be evaluated numerically as

$$\begin{aligned} F_X(x) &= E_{X_f} [F_{X_{\text{s,dB}}}(x - 10 \log_{10} X_f)] \\ &= \int_0^\infty \left[1 - \frac{1}{2} \operatorname{erfc} \left(\frac{x - 10 \log_{10} y}{\sigma\sqrt{2}} \right) \right] f_{X_f}(y) dy \end{aligned}$$

where the probability density function of X_f is

$$f_{X_f}(y) = \frac{m^m}{\Gamma(m)} y^{m-1} e^{-my}$$

and $\Gamma(\cdot)$ is the Gamma function.

Finally, to obtain the average outage probability over the entire coverage area, we must average (5) over the area of the cell. For uniformly distributed terminal locations in a cell bounded by radii R_{min} and R_{max} , it can be shown that this average is given by [6]

$$\overline{P_{\text{out}}} = \frac{1}{R_{\text{max}}^2 - R_{\text{min}}^2} \int_{R_{\text{min}}}^{R_{\text{max}}} P_{\text{out}}(r) 2r dr \quad (6)$$

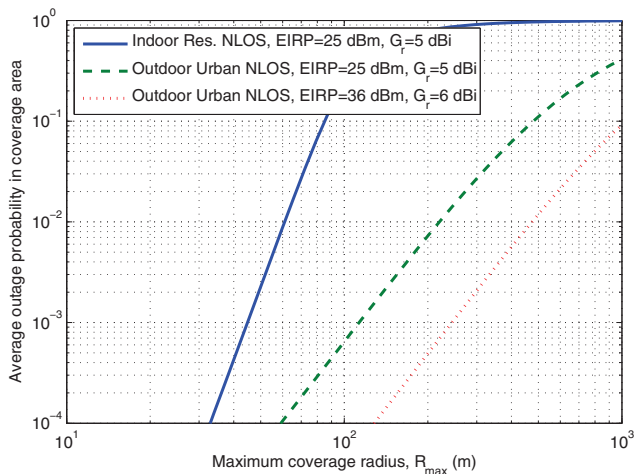


Fig. 4. Sample outage results at 2.4 GHz

TABLE III
PHY PARAMETER VALUES USED FOR FIG. 4

PHY Model Parameter	Symbol	Value
PHY data rate	R_b	1 Mb/s
Required E_b/N_0	$(E_b/N_0)_{\text{req,dB}}$	10.4 dB
Receiver noise figure	F	5 dB
Temperature	T_0	293 K
System losses	$L_{s,\text{dB}}$	1.5 dB

C. Example

Fig. 4 plots sample results for the average outage probability (6) as a function of the maximum coverage radius, R_{max} , and for $R_{\text{min}} = 10$ m. Outage curves for three cases are shown, all at 2.4 GHz: (i) the indoor residential non-line-of-sight (NLOS) environment (row 2 of Table II) at typical transmit power, (ii) the outdoor urban NLOS environment (row 4 of Table II) at typical transmit power, and (iii) the same outdoor environment but operating at the maximum permitted EIRP for the unlicensed 2.4 GHz band. In each case, the fading is Rayleigh (i.e., Nakagami fading parameter $m = 1$). The values for the remaining technology-specific parameters used in this example are listed in Table III and generally correspond to the IEEE 802.11 standard operating at 1 Mb/s.

Fig. 4 shows that, for this example, the outdoor coverage radius corresponding to a 1% outage probability is 220 m at moderate transmission power and nearly 500 m at maximum transmission power. Furthermore, the indoor range is clearly sufficient for most indoor residential environments.

V. LINK PERFORMANCE ANALYSIS: IEEE 802.11

Unlike the coverage analysis which is based on a generic model, a link performance analysis is typically based on a model that is specific to a MAC implementation. This section discusses link performance results using IEEE 802.11 as an illustrative example, as it has been thoroughly studied in the technical literature, and well-known approaches are available to model it. First, a model for the IEEE 802.11 MAC is briefly described, followed by a discussion of sample numerical results.

A. IEEE 802.11 Model Description

Our model of the IEEE 802.11 MAC layer is derived from Bianchi's seminal model [11], which developed a Markov chain representation for the state of a given station's backoff counter but which assumes that all stations are in saturation. Each terminal has a retransmission limit of α , and a frame is dropped after $\alpha + 1$ failed transmission attempts. Our model, described more fully in [4], uses several enhancements to the Bianchi model, including the use of probability generating functions and an M/M/1/K queueing model as proposed by Zhai et al. [12] to account for non-saturation and finite buffers.

Daneshgaran et al. [13] developed an extension to the Bianchi model that also eliminated the saturated station assumption. In addition, their model considered the possibility that a station could capture the channel and successfully transmit its frame, even during a collision event, provided that its power as received by the access point (AP) was sufficiently greater than that of the other stations. Our model also incorporates this capture effect, however rather than decouple the collision and channel capture from a frame loss due to channel effects, we consider them as statistically dependent events.

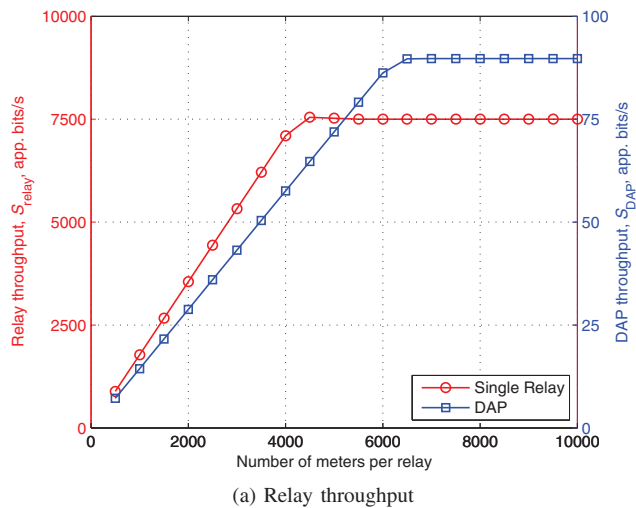
Finally, because the applications which we are considering result in traffic flows in both directions on every link in the network, we extended the Bianchi model to include traffic on the downlink from the AP to the stations and to account for half-duplex transmissions in both directions. A version of the half-duplex link model was developed by Jin et al. [14], but this model assumes that the stations and the access point are all in saturation. Our model allows for the stations to not be in saturation.

B. Numerical Results

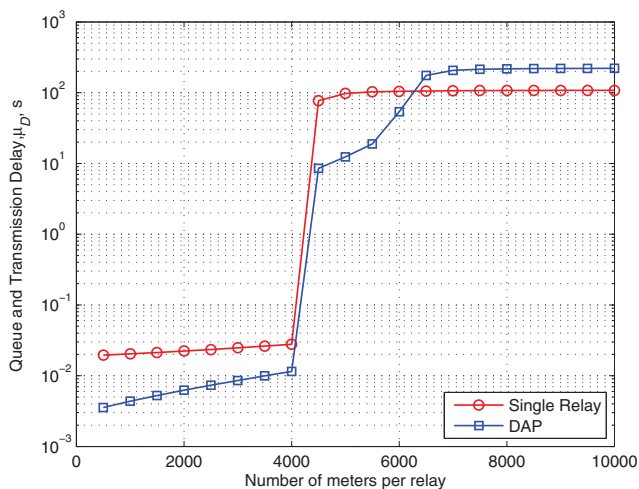
Consider the example logical link topology of the Smart Grid network illustrated in Fig. 3. The actors are grouped into Operations and Customer domains connected through DAPs. The AMI Headend has a link with multiple DAPs, each of which in turn has a link with multiple smart meters (SMs). The offered load on each link is listed in Table I.

For illustrative purposes only, the logical link between a DAP and the smart meters was analyzed assuming the use of an intervening layer of relays. The relays aggregate traffic from smart meters and send the aggregated traffic to the DAP over an IEEE 802.11 wireless multiple access network. Using the physical layer parameter values of Table III along with the channel parameters for the outdoor urban NLOS environment in Table II, our IEEE 802.11 analysis tool processed the traffic parameters of the DAP-relay link and returned the mean delay, reliability, and throughput of the uplink and downlink. The number of relays communicating with the DAP was set to 40 in this example, and the smart meters were assumed to be evenly allocated to the relays. Furthermore, we assumed each relay had a buffer that could hold 50 frames, and the DAP's buffer could hold 100 frames.

Fig. 5 plots the throughput and delay on the DAP-relay link as a function of the number of smart meters served by each relay. The relay-DAP uplink saturates first, because



(a) Relay throughput



(b) Mean delay of relay and DAP

Fig. 5. IEEE 802.11 link performance between a SM relay and a DAP, as a function of the number of SMs aggregated per relay

of its higher traffic load, but not until the number of smart meters per relay reaches 4000. Recalling the coverage analysis of Fig. 4, the coverage radius at maximum power and 1% outage probability is about 0.5 km. Assuming comparable DAP and relay coverage radii, and an urban meter density of 2000 electric meters per square kilometer, the DAP would only have about 6000 smart meters within its two-hop coverage area, or about 150 smart meters per relay, far below the link’s capacity limit of 4000 smart meters per relay. Thus, considering all factors—geographic coverage, traffic load, and link performance—we observe that the SM relay-DAP link in this example is coverage-limited, not bandwidth-limited, and therefore has excess network capacity.

The traffic load used in this example is based on three use cases described in [2]. Additional application traffic will cause the network to saturate at a lower number of meters.

VI. CONCLUSION

This paper presented a methodology to evaluate wireless technologies for the Smart Grid. We described an approach

to modeling wireless communications at the link layer that, first, identifies the various applications utilizing a specific link. Second, it translates the requirements of these applications to link traffic characteristics in the form of a link layer arrival rate and average message size. Third, it uses a coverage analysis to determine the maximum range of the technology under an outage constraint and for a given set of channel propagation parameters. Finally, using the link traffic characteristics and coverage area determined above, it employs a MAC/PHY model to measure link performance in terms of reliability, delay, and throughput.

As an illustrative example of the proposed modeling approach, we analyzed the wireless communications performance of three application use cases—service switch, meter reading, and plug-in hybrid electric vehicle—over an IEEE 802.11 link. Using appropriate MAC/PHY models, similar analyses can be performed for other wireless technologies.

REFERENCES

- [1] NIST SmartGrid Twiki: <http://collaborate.nist.gov/twiki-sgrid/bin/view/SmartGrid/PAP02Wireless>.
- [2] SG Network Systems Requirements Specification, v. 2.1, Mar. 12, 2010. Available online at http://osgug.ucauiug.org/UtiliComm/Shared%20Documents/Interium_Release_2/.
- [3] Boyer, W.F. and McBride, S.A., “Study of Security Attributes of Smart Grid Systems - Current Cyber Security Issues,” INL/EXT-09-15500, Idaho National Laboratory Critical Infrastructure Protection/Resilience Center, Idaho Falls, Idaho, Apr. 2009. Available online at <http://www.inl.gov/technicalpublications/Documents/4235623.pdf>.
- [4] D. Griffith, M. Souryal, C. Gentile, and N. Golmie, “An integrated PHY and MAC layer model for half-duplex IEEE 802.11 networks,” accepted for publication in *Proc. IEEE Military Communications Conf.*, Oct./Nov. 2010.
- [5] A. Papoulis, “Probability, Random Variables, and Stochastic Processes,” McGraw-Hill, Inc., Third Edition, 1991.
- [6] T. S. Rappaport, *Wireless Communications: Principles and Practice*. Upper Saddle River, New Jersey: Prentice Hall PTR, 1996.
- [7] C. Gentile, S. M. Lopez, and A. Kik, “A comprehensive spatial-temporal channel propagation model for the ultra-wideband spectrum 2-8 GHz,” in *Proc. IEEE Global Telecommunications Conf.*, Dec. 2009.
- [8] NIST UWB-MIMO Channel Propagation Measurements in the 2-8 GHz Spectrum. Available online at <http://www-x.antd.nist.gov/uwb>.
- [9] W. F. Young, K. A. Remley, J. Ladbury, C. L. Holloway, C. Grosvenor, G. Koepke, D. Camell, S. Floris, W. Numan, and A. Garuti, “Measurements to support public safety communications: Attenuation and variability of 750 MHz radio wave signals in four large building structures,” *Natl. Inst. Stand. Technol. Note 1552*, Aug. 2009.
- [10] D. W. Matolak, K. A. Remley, C. Gentile, C. L. Holloway, Q. Wu, and Q. Zhang, “Ground-based urban channel characteristics for two public safety bands,” submitted to *IEEE Trans. on Antennas and Propagation*, Dec. 2009.
- [11] G. Bianchi, “Performance analysis of the IEEE 802.11 distributed coordination function,” *IEEE Journal on Selected Areas in Communications*, vol. 18, no. 3, pp. 535–547, Mar. 2000.
- [12] H. Q. Zhai, Y. G. Kwon, and Y. G. Fang, “Performance analysis of IEEE 802.11 MAC protocols in wireless LANs,” *Wireless Communications and Mobile Computing*, vol. 4, no. 8, pp. 917–931, Dec. 2004.
- [13] F. Daneshgaran, M. Laddomada, F. Mesiti, and M. Mondin, “Unsaturated throughput analysis of IEEE 802.11 in presence of non ideal transmission channel and capture effects,” *IEEE Transactions on Wireless Communications*, vol. 7, no. 4, pp. 1276–1286, Apr. 2008.
- [14] H. Jin, B. C. Jung, H. Y. Hwang, and D. K. Sung, “A throughput balancing problem between uplink and downlink in multi-user MIMO-based WLAN systems,” in *Proc. IEEE WCNC*, pp. 1795–1800, Apr. 2009.